CONF-870804--47

ENCAPSULATED SINK-SIDE THERMAL ENERGY STORAGE FOR PULSED SPACE POWER SYSTEMS*

J. P. Foote
D. G. Morris
M. Olszewski
Engineering Technology Division
Oak Ridge National Laboratory
Oak Ridge, Tennessee 37831

CONF-870804--47

DE88 003917

Presented at the
22nd Intersociety Energy Conversion
Engineering Conference
Philadelphia, PA
August 10-14, 1987

*Research sponsored by the Air Force Wright Aeronautical Laboratories under Martin Marietta Energy Systems, Inc., contract DE-AC05-84OR21400 with the U.S. Department of Energy.

DISCLAIMER

ABSTRACT

Inclusion of thermal energy storage in a pulsed space power supply will reduce the mass of the heat rejection system. In this mode, waste heat generated during the brief high-power burst operation is placed in the thermal store; later, the heat in the store is rejected to space via the radiator over the much longer nonoperational period of the orbit. Thus, the radiator required is of significantly smaller capacity.

A candidate design for the thermal energy store component utilizes lithium hydride encapsulated in 304L stainless steel or molybdenum in a packed-bed configuration with a lithium or sodium-potassium (NaK) heat transport fluid.

Preliminary thermal analysis indicates that, for lithium hydride in a sphere of 4-cm maximum diameter, complete lithium hydride melting will be achieved in 500 s; this provides a subunit with maximum energy storage density. However, an elastic stress analysis indicates that the stresses generated in a rigid spherical shell by the melting lithium hydride will necessitate a thick shell, significantly reducing the energy storage density. This may be mitigated by cracks which form in the lithium hydride during cooldown, providing channels for flow of the melting salt during the charge cycle.

Initial scoping experiments with encapsulated lithium hydride have been completed with cylindrical and spherical containers. Four thermal cycles were completed without shell failure with a cylindrical container with a 0.0889 cm (35-mil) wall thickness A 0.0254 cm (10-mil) thick spherical container successfully completed one thermal cycle. Post-test examination of all containers tested showed the presence of numerous cracks in the lithium hydride.

1. Introduction

In sprint mode space applications, which require high power for relatively short durations, energy storage devices may be employed to reduce the size and mass of the thermal management system. This is accomplished by placing the reject heat (from the primary power system or other system components) in the thermal store during the sprint mode. During the remaining nonoperational portion of the orbit, which can be an order of magnitude longer than the sprint period, the stored heat is dissipated to space. The heat rejection rate is thus reduced, and this results in a smaller radiator being required. In concepts that are constrained by launch volume or deployed projection area, this can

be a critically important attribute. Additionally, if the reduction in radiator mass is greater than the additional storage mass, overall system mass savings are possible.

Lithium hydride (LiH) has been identified as the best candidate for use in power system sink-side thermal energy storage applications due to its superior heat storage properties and suitable melt temperature (T_m = 962K). To maximize storage density, both sensible and latent modes of heat storage are used.

This paper focuses on the use of encapsulated lithium hydride shapes in a packed bed storage unit with lithium or NaK as the heat transport fluid. Analytical and experimental development work associated with the concept is described. Since the program is in its early stages, emphasis thus far has been on feasibility issues associated with encapsulating lithium hydride spheres. These issues include shell stress induced by phase-change during heating, hydrogen diffusion through the encapsulating shell, heat transfer limitations due to poor conductivity of the salt, void behavior, and material constraints. The impact of these issues on the design of encapsulated lithium hydride spheres has been evaluated, and design alternatives have been identified for circumventing key problem areas.

2. System Concept Analysis

System value analysis was performed to determine, in a preliminary manner, the minimum storage density required for the encapsulated lithium hydride packed-bed storage concept to be feasible. A scoping design analysis was then conducted to determine the design conditions necessary for the storage unit to meet the required storage density.

These design requirements were then used to set the goals for the development effort.

Value Analysis

A simplified schematic of a no-effluent space power system employing an encapsulated lithium hydride packed-bed for sink-side thermal storage is shown in Fig. 1. Depending upon the application, the source could be nuclear, solar, or chemical. Power conversion could be accomplished using dynamic system such as Brayton or Rankine cycles or static systems such as thermionics. Engineering details necessary to integrate the storage system with the various power conversion options have not been delineated and are beyond the scope of this study. However, it appears that thermionic conversion may be best suited to accommodate variable temperature storage.

Previous analysis[1] identified and examined the major parameters affecting the value of storage and demonstrated that the optimum storage minimum temperature was in the 500 to 700 K range. Thus, the value analysis performed to set research goals was limited to this range for the lower operating temperature of the store. The crossover time, plotted in Fig. 2 as a function of storage density, is defined as the time at which the storage and radiator-only systems are of equal mass. For generation times less than the crossover time the storage system is lighter (the benefit of storage increasing as the generation time decreases). To have reasonable applicability to sprint power needs it was decided that a crossover time of at least 500 s would be desirable. Thus, the minimum system storage density was fixed at 3 MJ/kg.

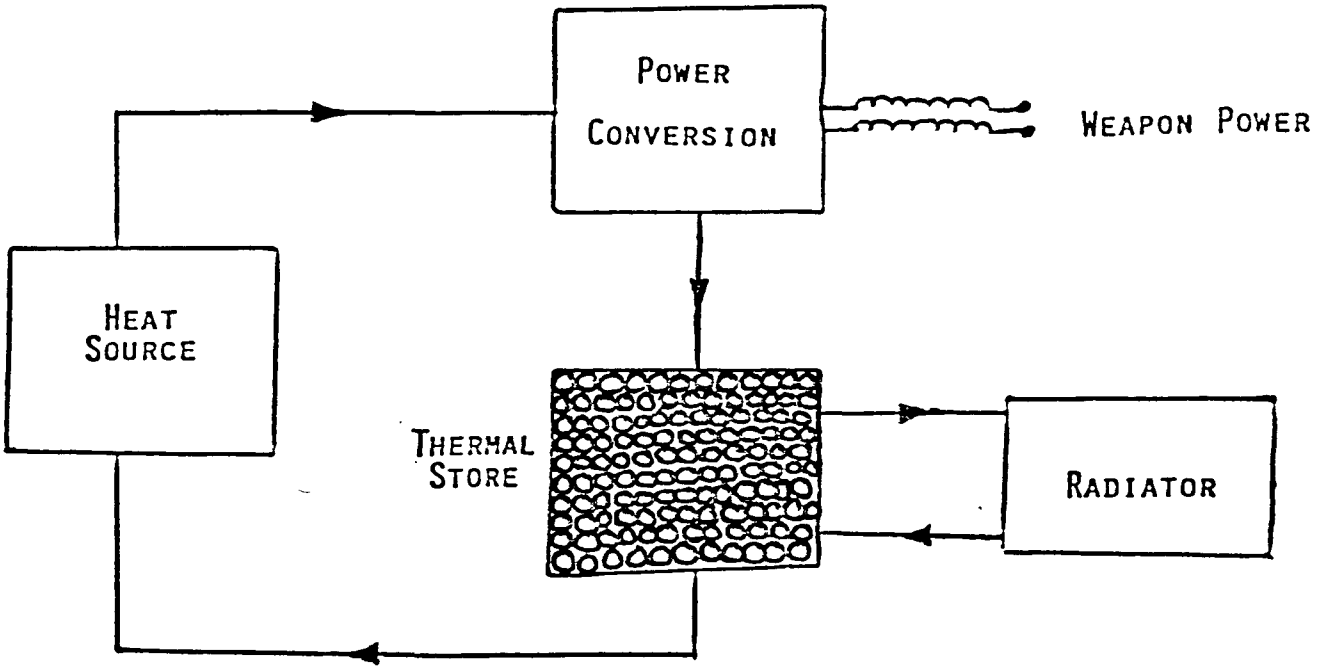

Simplified

Fig. 1. Schematic of power system employing encapsulated sink-side thermal storage.

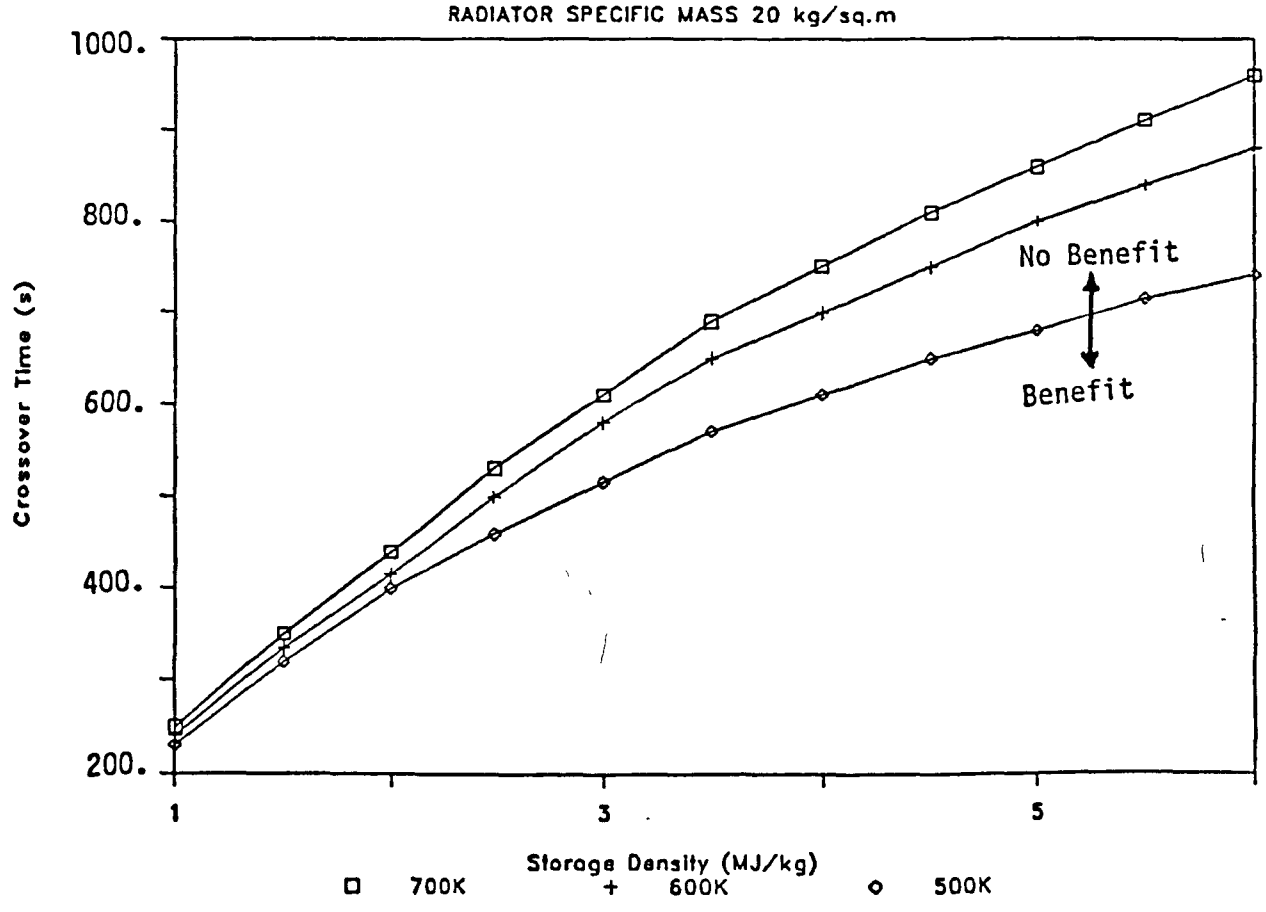

Fig. 2. Heat rejection system crossover time for selected minimum storage temperatures.

Storage System Conceptual Design

Preliminary system conceptual designs were prepared for the proposed packed bed storage system. System storage densities were calculated for several design options. Lithium and NaK were examined as the heat transport fluids. Also, the storage medium was examined using naturally occurring lithium (Li-7) and the isotope Li-6. Preliminary information indicates that Li-6 possesses the same molar properties as Li-7. Thus, on a mass basis the heat of fusion and specific heat will be 12% higher for Li-6. It was assumed that the lithium hydride spheres were encapsulated with a 0.013-cm (5-mil) thick stainless steel shell (this represents a design goal). The heat transport properties of lithium hydride limited the maximum sphere diameter to 3.8 cm (the maximum diameter that allows for complete melting of the lithium hydride).[2] With this design the shell accounted for about 22% of the sphere mass. Packing densities of 60 and 75% were also examined.

As indicated by the results of the design analysis (see Table 1), lithium is the preferred thermal transport fluid since all designs yield system storage densities in excess of 3 MJ/kg. Not surprisingly, the use of Li-6 is also preferred because of its enhanced storage density. Thus, it was concluded from the analysis that the design goal for the encapsulating shell should be fixed at 0.013 cm for spheres with a diameter of 3.8 cm.

Table 1. Storage system operational energy densities (MJ/Kg)

Minimum store temperature (K)	LiH only		Encapsulated							
			Li-7				Li-6			
			75%		60%		75%		60%	
	Li-7	Li-6	NaK	Li	NaK	Li	NaK	Li	NaK	Li
300.	7.90	9.04	4.46	5.32	3.70	5.02	4.78	5.76	3.91	5.37
400.	7.44	8.51	4.20	4.99	3.47	4.68	4.50	5.40	3.67	5.01
500.	6.96	7.96	3.92	4.65	3.23	4.34	4.21	5.03	3.42	4.64
600.	6.42	7.34	3.62	4.27	2.97	3.96	3.88	4.62	3.14	4.23
700.	5.80	6.63	3.27	3.84	2.68	3.53	3.51	4.16	2.83	3.78

3. Development Issues and Evaluation

Thermal Assessment

Heat Transfer Model. A two-dimensional finite difference heat transfer computer code is being developed to model the thermal performance of lithium hydride encapsulated in a spherical shell. The model uses the "enthalpy" method to account for phase-change in the salt. In the enthalpy method, the location of the phase-change front is not determined directly but is inferred from the energy content of the material. The computer program solves the fully implicit form of the heat balance equations. The fully implicit formulation is used to avoid stability problems associated with the explicit solution and to minimize the difficulty in implementing a natural convection model. Heat balance equations are solved on a regular grid in r, θ coordinates. The equations are solved directly for the one-dimensional case or by line relaxation for the two-dimensional case. The solution method is given in Ref. 3. Temperatures are scaled so the scaled temperature, T', at the melt point is zero:

$$T' = T - T_{MP} ,$$

where

$$T_{MP} \approx 962 \text{ K}$$

Energy content is scaled so the energy content, E, of the solid at the melt point is zero. Therefore,

$$E = C_S T' \qquad \text{For } T' < 0$$

$$E = C_L T' + H_{SL} \qquad \text{For } T' > 0$$

where C_S and C_L are the specific heats of the solid and liquid, and H_{SL} is the heat of fusion (≈ 2.85 MJ/kg). When a given node has $0 < E < H_{SL}$, the temperature is fixed at zero until enough heat is added or removed so $E > H_{SL}$ or $E < 0$.

Results from the finite difference model were compared to an analytical solution for a one-dimensional, constant density Stefan problem for a sphere.[4] Results of two-dimensional calculations were checked against results from the explicit HEATING6 code. HEATING6 is a general purpose heat transfer program commonly used at ORNL. Agreement was satisfactory in both cases.

Heat Transfer Analysis. The finite difference code was used to determine the thermal response of single spheres of various diameters exposed to liquid metal convection when the fluid temperature undergoes a step change from 300 to 1100 K. This simulates heat rejection to the packed-bed during the sprint mode. Based on theoretical relationships for liquid metal flowing past a single sphere,[5] an average convection coefficient of 17 KW/m^2-K was used for spheres in a packed-bed.

The mass of lithium hydride in the spheres was set so they are completely filled when the lithium hydride is liquid. The shells are stainless steel, with thickness equal to 1% of the inside radius [e.g., for IR = 1.9 cm, shell thickness = 0.019 cm (7.5 mil)]. Linear scaling of shell thickness can be justified due to stress considerations, and as

a result the shell has no effect when comparing the specific energy content of different size spheres. Properties for the shell material, and solid and liquid lithium hydride were considered to be constant.

In order to formulate a thermal model for melting of lithium hydride in a sphere, two important assumptions must be made. The first of these is the initial location of the void in the solid material. The behavior of the void during solidification is not well understood, and developing an understanding of void mechanics is one of the main goals of this project. However, analysis indicates that in the case of uniform cooling in micro-gravity, a spherical void will form in the center of the container.[2] This assumption is made in the present study. The second critical assumption concerns how the volumetric expansion due to melting is accounted for in the case where the liquid is not in contact with the void. The first possibility is that the shell expands to provide the required volume. This case is not of interest in the heat transfer study, since any practical shell would be able to expand very little before rupturing. It is, however, of great interest in determining the design of the shell. A second way the volume expansion could be accommodated is for the solid to be crushed inward into the void. Whether or not this is a realistic possibility with a practical shell thickness depends on the compressive strength of the solid lithium hydride, but in any event it provides a limiting case for the heat transfer study. A third possibility is for the excess liquid to leak through the solid into the void. This would likely occur if there are cracks in the solid. Heat transfer calculations were carried out assuming the second case mentioned above, referred to as the "crush"

model, and the latter case, referred to as the "leak" model. In the leak model calculations, the means by which the liquid makes its way through the solid is not considered. It is assumed that liquid at the fusion temperature appears in a freezing volume at the inner surface of the solid.

During the early stage of the melting process, the two models give very similar results, but as the process continues the rate of melting predicted by the leak model begins to exceed that of the crush model. This difference increases with time. This result is due primarily to two effects. The conduction path through the liquid is shorter in the leak model. In addition, some heat is carried along with the liquid that leaks through the solid and thus bypasses the conduction path through the solid.

Figure 3 shows a comparison of energy gain versus time for spheres ranging from 0.635 to 3.81 cm in radius. Assuming a total time of 500 s available for charging, the 1.9 cm radius sphere is the largest that attains its maximum potential energy storage in the required time. The 3.81 cm radius sphere requires about 900 s to completely melt. Table 2 lists energy content after 500 s for the various sphere sizes predicted by the crush and leak models. It is interesting to note that the results for the two cases do not differ greatly (the maximum difference is about 2%).

In summary, the mechanism by which the volume expansion due to melting is accommodated is not critical in the heat transfer model. Both models indicate that for complete melting in 500 s with an 1100 K

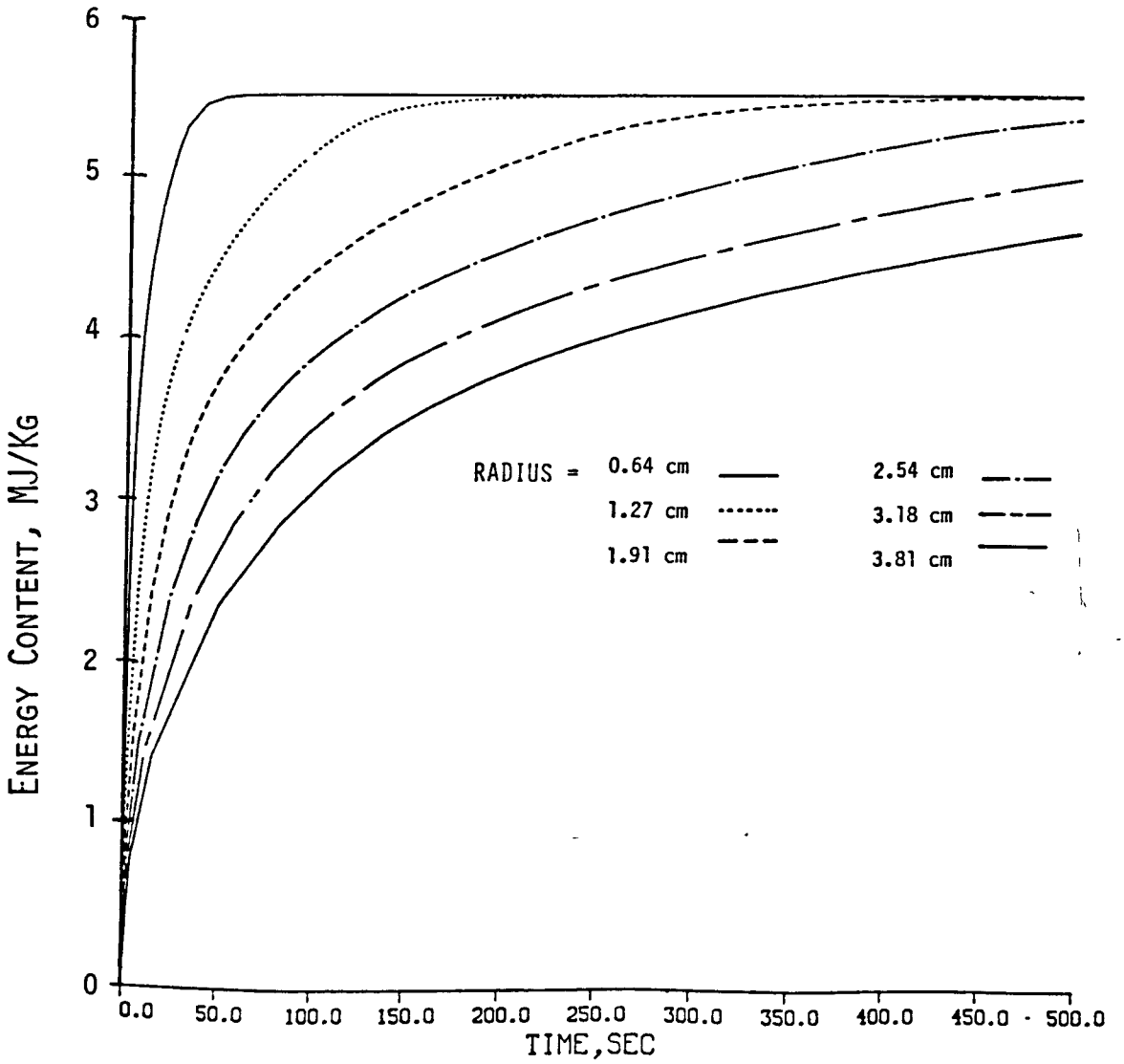

Fig. 3. Energy storage versus time for spherically encapsulated lithium hydride (leak model).

Table 2. Energy content at 500 s
for various sphere sizes

Radius		Energy content at 500 s			
		Crush model		Leak model	
(cm)	(inches)	(MJ/kg)	(% max)	(MJ/kg)	(% max)
0.64	0.25	5.560	100.0	5.559	100.0
1.27	0.50	5.558	99.96	5.558	99.98
1.91	0.75	5.532	99.50	5.550	99.84
2.54	1.00	5.260	94.60	5.412	97.36
3.18	1.25	4.918	88.45	5.039	90.65
3.81	1.50	4.611	82.93	4.701	84.57

source temperature, the maximum container diameter that can be used is about 3.8 cm.

Phase-Change Induced Shell Stress

As mentioned previously, the void is expected to be located in the sphere center following cooldown in a micro-gravity space environment. Then, during heatup, the liquid lithium hydride expands against the shell and solid lithium hydride. Figure 4 presents calculated shell temperature, average lithium hydride solid temperature, and minimum solid lithium hydride temperature as a function of time for a 3.8 cm diameter sphere with an initial temperature of 700 K suddenly exposed to liquid metal at 1100 K. The curves were generated using the one-dimensional "crush" model. It can be seen that while the shell reaches the liquid metal temperature very rapidly, much of the solid is at a temperature significantly below the melt point when the lithium hydride adjacent to the shell starts to melt.

A simple elastic stress analysis was performed to determine, in an approximate manner, the required shell thickness to prevent shell rupture. Molybdenum and 304L stainless steel were evaluated to determine the minimum required shell thickness. In this analysis the following assumptions were made:

1. the void forms in the sphere center,
2. the lithium hydride forms a thick shell with no cracks,
3. the containment shell is a thin shell, and
4. thermal stresses other than those resulting from phase-change are neglected.

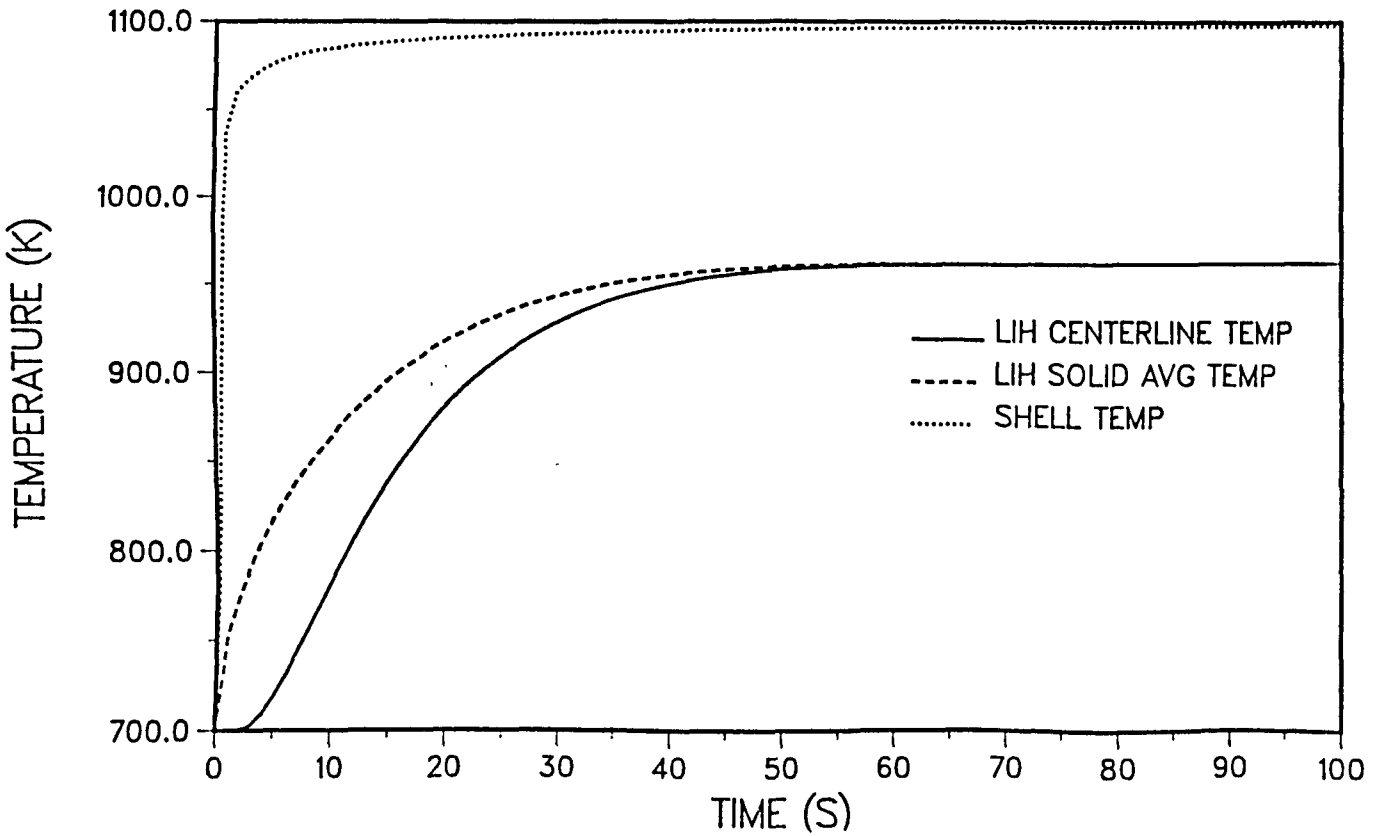

Fig. 4. Temperature profiles in spherically encapsulated lithium hydride during the charge cycle.

In addition, based on the thermal profiles in Fig. 4, the containment shell was assumed to be isothermal at the peak operating temperature, and the solid lithium hydride was assumed to be isothermal at the minimum storage temperature.

As shown in Ref. 2, the minimum required shell thickness to prevent rupture is given by:

$$t = r/3\ (\sigma_{LiH}/\sigma_S)(\rho_L/\rho_S) \quad ,$$

where

r = sphere radius

σ_{LiH} = LiH compressive strength

σ_S = shell tensile strength

ρ_L, ρ_S = density of liquid and solid LiH.

Pressed lithium hydride ultimate compressive strength data are given in Fig. 5 (left vertical axis). As shown there is a strong temperature dependence.[6,7] Table 3 presents lithium hydride compressive strength at room temperature for pressed and sintered material.[8] These data indicate that sintering results in large strength gains (about a factor of 1.7 greater for the 10 cycle sample). The sintered data are more likely representative of cast material, thus the data of Fig. 5 should probably be scaled upward by this factor. This has been done in the right vertical axis of Fig. 5.

At ~1100 K, the yield strength of 304L stainless steel[9] and molybdenum[10] are taken as 69 (estimated) and 255 MPa (10 and 37 ksi), respectively. These properties do not reflect any effects of hydrogen or

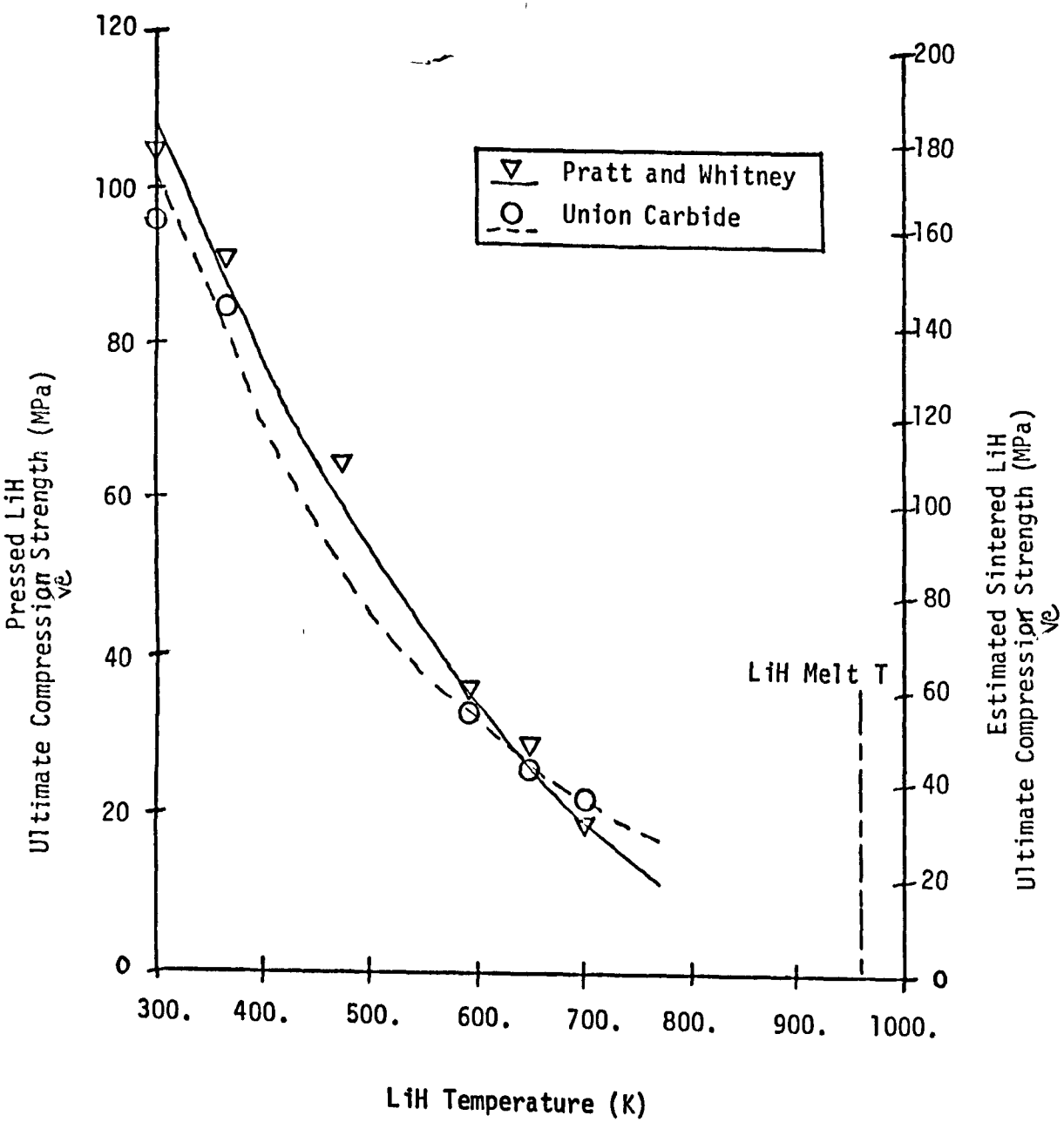

Fig. 5. Pressed and estimated cast lithium hydride ultimate compression strength (Refs. 6, 7).

Table 3. Compressive strength of lithium hydride at room temperature (Ref. 8)

Strength		Comments
MPa	psi	
100.7 ± 3.34	14,600 ± 485	Cold pressed
135.6 ± 34.61	19,670 ± 5,020	Cold pressed and sintered, 3 cycles*
110.0 ± 30.13	15,950 ± 4,370	Cold pressed and sintered, 5 cycles*
167.5 ± 6.31	24,300 ± 915	Cold pressed and sintered, 10 cycles*
	(95% confidence interval - room-temperature data)	*Blocks thermal cycled from room temperature to 593°C, specimens machined from sound, uncracked portion of blocks

lithium on strength; however, for short lifetimes these effects are expected to be small.

Calculated achievable energy storage densities (i.e., includes shell and lithium hydride) based on the minimum required shell thickness determined as described above are presented in Table 4 for encapsulated lithium hydride in spherical shells constructed of 304L stainless steel and molybdenum. Storage densities are based on a 500 s heatup period and use of naturally occurring lithium and are shown for a range of minimum storage temperatures. These results show that the required shell thickness is very large at low minimum storage temperatures, reflecting high lithium hydride compressive strength. Obviously, with thick shells, only a very low energy storage density can be achieved. Even for minimum storage temperatures in the 500 to 700 K range, calculated shell thicknesses are much greater than permitted to obtain desired energy storage densities. As the lithium hydride melt temperature is approached and the lithium hydride strength is reduced, more reasonable shell thicknesses and energy storage densities can be achieved. For comparison purposes, energy storage with lithium is shown in Table 4 where it is assumed that a shell with negligible mass can be used. In the operating range of interest for the minimum storage temperature (500 to 700 K), the achievable storage density is still well below that desired.

The storage densities presented in Table 4 can be compared to those shown in Table 1 for ^{6}LiH and ^{7}LiH, alone, to see the penalty paid for the encapsulating shell or using lithium instead of lithium hydride.

Table 4. Energy storage densities of lithium hydride (stress constrained) and lithium

Minimum store T (K)	Molybdenum shell			Stainless steel shell			Li (no shell) energy storage density (MJ/kg)
	Required shell thickness (cm)	(mils)	Energy storage density (MJ/kg)	Required shell thickness (cm)	(mils)	Energy storage density (MJ/kg)	
300	0.29	116	0.90	1.08	426	0.50	3.7
400	0.23	92	1.0	0.86	338	0.51	3.3
500	0.17	67	1.2	0.62	246	0.57	2.5
600	0.097	38	1.7	0.35	139	0.77	2.1
700	0.069	27	1.9	0.26	101	0.88	1.7
800	0.043	17	2.3	0.15	61	1.1	1.3
900	0.013	5	3.1	0.051	20	2.0	0.84
962	0.0020	0.8	3.6	0.0076	3	3.0	0.56

Note: Sphere diameter = 3.81 cm.

LiH mass ≈ 15.5 grams

Pulse duration = 500 s

Natural lithium

Based on elastic stress analysis it appears that a desired shell thickness of ~0.0127 cm (5 mil) cannot be obtained in the temperature range of interest (even for a molybdenum shell, a material with substantial high temperature strength) if lithium hydride forms a monolithic shell.

However, it has been observed in tests conducted for this program and others,[11,12] that cracks form in the lithium hydride during cooldown. Thus, cracks that penetrate the solid lithium hydride from the containment shell to the void, may provide a path for expanding liquid lithium hydride to reach the centrally located void during heatup. Hence, large hydrostatic forces are avoided, and a thin shell can successfully contain the lithium hydride.

In the event that predictable, "well-behaved" cracks do not form, there are a series of potential design modifications to mitigate the stress problem. The following modifications have been investigated:[2]

1. providing internal fins made of the shell material,
2. using a non-wetting container material/coating or insulating part of the container surface, thus causing the void to form at the wall, and
3. making the container flexible.

Analysis indicates that the thermal conductivity of fins would have to be near that of copper to significantly affect heat transfer. However, fins may reduce the strength of the lithium hydride shell by breaking-up the monolithic structure.

It is suspected that controlling the wetting behavior would be difficult. Analysis indicates that insulating a portion of the sphere slows the freezing process in the area of the insulation; however,

further analysis is required to determine the influence of the void as the process progresses.

Thin-wall (~3.5 mil) bellows containers hold promise as a flexible container.

Although buckling of the shell due to the contraction of lithium hydride during cooldown is a potential concern, no buckling analysis has been performed. Analysis would be of questionable value since buckling is sometimes observed experimentally at only 10% of the predicted critical stress level. As described subsequently, buckling concerns have been alleviated to some extent due to successful thermal cycle testing of a thin-wall sphere.

Hydrogen Diffusion

Lithium hydride tends to dissociate into lithium and hydrogen gas as it is heated. To prevent lithium hydride dissociation an overpressure of hydrogen is required. Free hydrogen diffuses through the shell and results in a loss of energy storage density. As described in Ref. 13, hydrogen diffusion (loss) can be calculated using the following equation:

$$h_2 \text{ loss} = \frac{S\ t\ A\ P^{1/2}}{d},$$

where

S = hydrogen permeability of the metal,

t = time,

A = surface area of the encapsulating metal,

P = hydrogen pressure, and

d = shell wall thickness.

The hydrogen permeabilities of clean 304L stainless steel and molybdenum at 760 mm Hg and ~1100 K are approximately 0.45 and 0.07 CC(STP) mm/h-$atm^{1/2}$-cm^2, respectively.[13] Using these permeabilities, hydrogen loss from lithium hydride encapsulated in 304L stainless steel and molybdenum has been calculated for a 25 cycle lifetime.[14] The calculations were performed for a sphere with a diameter of 3.81 cm containing approximately 15.5 grams of lithium hydride (initial mole fraction 99.16%). In addition, calculations assumed the use of naturally occurring isotopic lithium hydride, a thermal storage temperature range of 700 to 1100 K, and a pulse duration and orbit time of 500 and 5880 s, respectively. Phenomenologically, it was assumed that hydrogen diffusion occurred, calculated as previously described, when liquid or hydrogen gas contacted the container wall, and that on cooldown lithium hydride freezes first and uniformly on the shell surface preventing further hydrogen diffusion (i.e., the lithium hydride freezes over the entire shell surface which ultimately results in a central void).

Based on the assumptions described above, Table 5 presents the calculated loss in energy storage density for molybdenum and clean stainless steel shells 0.00254, 0.0127, and 0.0381 cm (1, 5, and 10 mils) thick. These calculations indicate that hydrogen loss through a 0.0127 cm (5 mil) clean stainless shell results in only a 2.9% storage density loss; however, the loss associated with a 0.00254 cm (1 mil) thick clean stainless steel shell is relatively high at 11%. On the other hand,

Table 5. Effect of hydrogen loss on energy storage density

Shell thickness (cm)	(mil)	Material	Energy density (MJ/kg)		Energy density loss (%)
			1st cycle	25th cycle	
0.00254	1	SS-clean	5.468	4.880	11.
0.0127	5	SS-clean	4.493	4.362	2.9
0.0381	15	SS-clean	3.112	3.068	1.4
0.00254	1	Molybdenum	5.379	5.250	2.4
0.0127	5	Molybdenum	4.206	4.173	0.78
0.0381	15	Molybdenum	2.725	2.715	0.37

molybdenum shells as thin as 0.00254 cm (1 mil) can be used with less than 3% loss in storage density.

Material Considerations

Successful encapsulation of lithium hydride requires that the shell material be compatible with lithium hydride, lithium and hydrogen since all three materials will be present in the capsule. Compatibility is required over the temperature range ~700 to 1100 K, where most of the exposure is at ~700 K. As mentioned previously, since the system is expected to be cycled 25 times over its lifetime, relatively short life is required at high temperatures (i.e., above the lithium hydride melt temperature).

Based on a review of relevant materials data from a variety of sources, it was concluded in Ref. 2 that 304L stainless steel and molybdenum are the leading candidate shell materials. Material considerations included material compatibility between the shell and lithium hydride, lithium, and hydrogen, ductility, strength, density, material cost, and ease of fabrication. The refactory metals niobium, tantalum, titanium, and zirconium have been eliminated from consideration due to hydrogen embrittlement. It was determined that silicon carbide (SiC) is not compatible with lithium at ~1100 K. Other ceramic materials have been eliminated primarily due to their brittle nature, and thus limited thermal shock resistance, and inability to permit even small stains without rupture which may occur during the initial period of phase-change on heatup. 304L stainless steel and molybdenum possess reasonable ductility and moderate density. Molybdenum has greater

strength and better material compatibility than 304L stainless steel, but is more expensive to fabricate.

4. Experimental Investigation

Scoping Experiments

Initial scoping experiments have been performed using 304L stainless steel cylindrical cans and a spherical can containing lithium hydride. The purposes of these experiments were to perform preliminary scoping tests of cylindrical and spherical containments and to gain experience in the thermal cycling of encapsulated lithium hydride. The tests provided insights into container (and weld) survivability following phase-change and the location and shape of the void formed during lithium hydride solidification. In addition, experience was gained in the areas of hydrogen gas evolution due to impurities and lithium hydride decomposition, furnace equipment functioning, and the thermal response of furnace and sample.

A "fill-tube" attached to the top of each can permitted pressure monitoring. The fill-tube was connected through flexible tubing to a pressure gage, vacuum pump, and argon purge line. The lithium hydride container was placed in a stainless steel beaker and packed with MgO. A thermocouple was located adjacent to the outside of the lithium hydride container about halfway up the side. The beaker was placed inside a small resistance heated furnace (~720 W) and the top of the furnace was covered with insulation. The cans were filled with preoutgassed lithium hydride powder (chemical analysis of similar samples indicated 99.16 mole % LiH).

Using the setup described above, three cylindrical can tests were performed. Two tests used cans of 2.54-cm length, 3.81-cm diameter, and 0.089-cm (35-mil) wall thickness, filled with about 14 grams of lithium hydride. Based on density considerations, containers would be ~90% full at the maximum anticipated experimental temperature (~1050 K). In the first test (test C-1), the can was cycled once from room temperature to ~1000 K and then back to room temperature. In the second test (test C-2), the can was cycled a total of four times over a two day period with two cycles performed each day. The second cycle performed each day was initiated from about 25 K below the melt point rather than after return to room temperature. Based on thermal analysis and thermocouple response, it is fairly certain that complete freezing occurred after completing the first cycle. Heating from about 25 K below the melt point to about 50 K above the melt point occurred over 1 h; the cooling process was also 1 h in duration.

Since the powder was preoutgassed, it was anticipated that only a small amount of gas would be evolved on heatup to the melt temperature. In all tests, this was observed. In heating through and above the phase-change temperature, the pressure rose in tests C-1 and C-2 to a maximum of about 100 mmHg. Based on peak temperatures achieved in the tests, high mole fraction of lithium hydride, and limited free volume, one would have expected to measure a much higher pressure. However, post-test examination revealed that the lithium hydride had "crawled" up the fill-tube and possibly isolated the lithium hydride in the can from pressure measurement. In test C-2, the lithium hydride had crawled through the fill-tube and entered the flexible tubing (lithium hydride

only partially filled the fill-tube in test C-1). The mechanism for this behavior is not currently understood, but is being investigated.

Post-test examination of the cycled test C-1 and C-2 canisters showed that a single, continuous void formed near the top of the can in both tests. As shown in Fig. 6, the void in the test C-1 can was not symmetrically formed, suggesting that the can was not level during testing and/or that there existed some nonuniform heating/cooling. Radiographs of the test C-2 can showed a similar void shape and location.

Comparison of measurements of container diameter before and after tests C-1 and C-2 showed no measurable change. However, comparison of before and after top-to-top measurements for test C-2 showed that the top-to-top distance had decreased about 0.05 cm (20 mil) (similar data was not collected for test C-1). Since the top and bottom of the can were flat, these surfaces could easily be deformed, possibly by "gripping" or shrinkage forces generated by the lithium hydride during cooldown. As a result of heating in an air atmosphere, cans in both tests oxidized. Based on visual observation, the welds performed without failure.

Test C-3 was performed with a cylindrical can with the same dimensions as those used in the first two tests, except that the wall thickness was 0.064 cm (25 mils). The primary objective of the test was to examine void behavior in a "hot-full" container (i.e., the can was filled with 16 grams of lithium hydride to produce a can almost completely full of liquid at the highest temperature anticipated). Experience with lithium fluoride at TRW[15] and ORNL[16] indicates that in some cases voids tend to be located near the center of the container

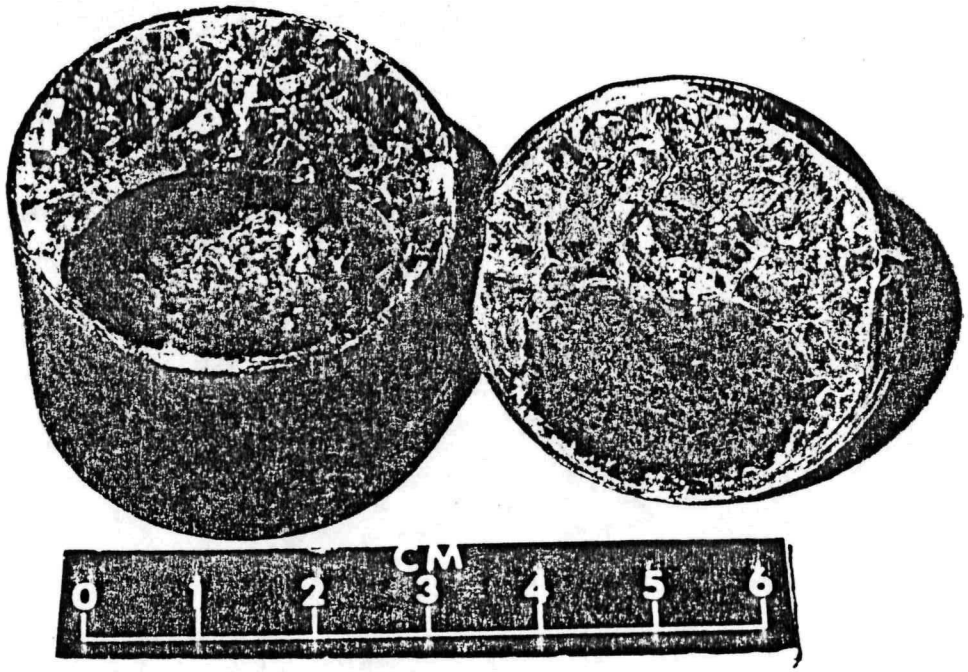

Fig. 6. Opened test C-1 cylindrical can following thermal cycle.

following solidification even in the presence of Earth's gravity. Test C-3 was conducted in a similar fashion to Test C-1 with one cycle being performed from room temperature to ~1000 K and then back to room temperature. Due to a can leak, an experimental determination of void behavior in a full can was not obtained. The leak apparently occurred at a weld point(s) where the top of the can was welded to the lid. This failure was not too surprising since the can was virtually completely full of powder when the weld was made. The weld was made with some difficulty as lithium hydride melted and made contact with the welded surfaces. During the test lithium hydride leaked into the MgO and crawled up the fill-tube resulting in a significant loss of lithium hydride from the can. Apparently, the lithium hydride was able to crawl up the can walls and exit through the opening(s) where the weld failure(s) occurred.

In a second attempt to examine void shape in a hot-full container, a spherical container with a 4.6-cm diameter and 0.0254 cm (10-mil) wall thickness was used. Two additional thermocouples were used in the test (test S-1). One was located in the fill-tube, about 5 cm above the top of the sphere, while the other thermocouple was positioned inside the sphere to measure the lithium hydride temperature. The sphere was heated through one thermal cycle. Shortly after apparently melting all of the lithium hydride, the tube thermocouple temperature rose 53 K over a 5 min. period (while the other temperature readings changed slightly) indicating lithium hydride crawling up the ~0.64 cm inside diameter tube (tube diameter for sphere test was much larger than cylindrical can tests). Based on post-test radiographs, the resulting void shape is

sketched in Fig. 7. As shown, the void formed in the top of the sphere. It can also be seen that lithium hydride crawled up the fill-tube. The effect of the fill-tube and lithium hydride crawling on the void shape and location is not known, but will be resolved in future sealed tests.

Post-test examination revealed no container deformation, thus indicating that a thin-wall sphere resists buckling due to lithium hydride contraction on cooldown.

In all tests conducted for this program, extensive cracking was observed (visually or radiographically) in the cast lithium hydride after cooldown (for example, see Fig. 6), and is most easily seen in radiographs.

In order to compare results of experiments conducted in normal gravity with heat transfer model predictions, void mechanics and natural convection models must must be integrated into the heat transfer model. The void influences the freezing pattern by causing some areas of the freeze front to "dry out". The liquid vapor interface also provides a boundary condition for the natural convection problem. In addition, the void reduces heat transfer at the container surface if it is located at the wall. The equilibrium liquid-vapor interface shape can be calculated for an axisymmetric case as a function of the surface tension, liquid density, gravity level and angle of contact between the liquid and container wall, based on a vertical force balance on the interface.[2] The freezing problem can then be solved without great difficulty, as it has been found that the liquid rapidly becomes isothermal at the fusion temperature when freezing begins. Thus the liquid can be

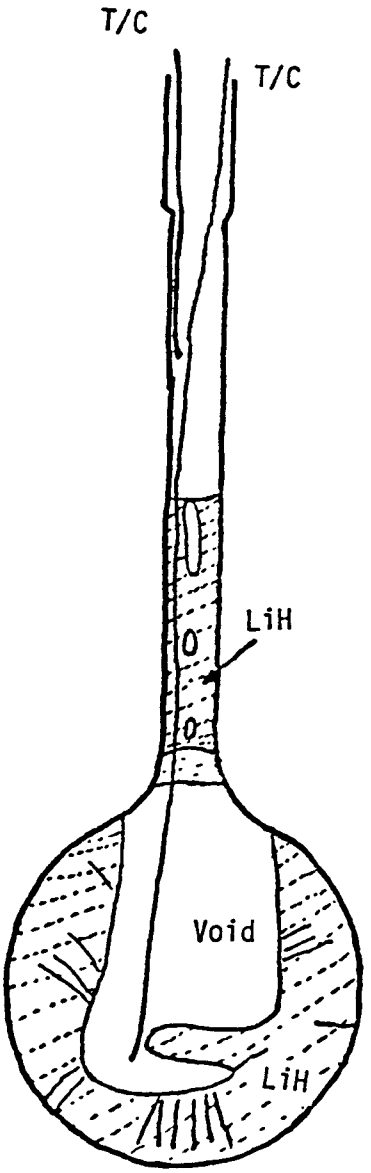

Fig. 7. Sketch of lithium hydride freeze pattern observed in spherical container test S-1.

treated as a lumped mass, and it is only necessary to determine which areas of the freeze front remain in contact with liquid to solve for the freezing pattern. Figure 8 shows the predicted distribution of frozen lithium hydride for a slowly cooled 4.6 cm diameter spherical container under normal gravity. The calculations were carried out using the static liquid-vapor interface shape and assuming the liquid to be a lumped mass. Aside from the crawling behavior, model results are consistent with experimental observation (Fig. 7).

Simplifications used in modeling the freezing process cannot be employed in the melting case, as most of the heat transfer is through the liquid. Natural convection will strongly influence the heat transfer, so the equations of motion must be solved in the liquid. A solution procedure based on the SIMPLE method developed by Patankar[3] is being incorporated into the model. Boundary conditions at the free surface are of particular importance in the fluid flow model, since the boundary conditions drive the flow in the micro-gravity case.

Development of High Heat Rate Furnace

Comparison between the capsule experiments performed thus far and conditions anticipated in the "real system" show some very important differences, other than the obviously small number of cycles experimentally performed. As indicated previously, operational heatup times from ~700 to 1100 K will be on the order of 10 min, whereas the laboratory procedure required hours.

In order to obtain real system heatup times, an existing Y-12 Plant graphite induction furnace will be modified and used for cycle testing. The furnace is cylindrical with a peak operational power of about 60 kW,

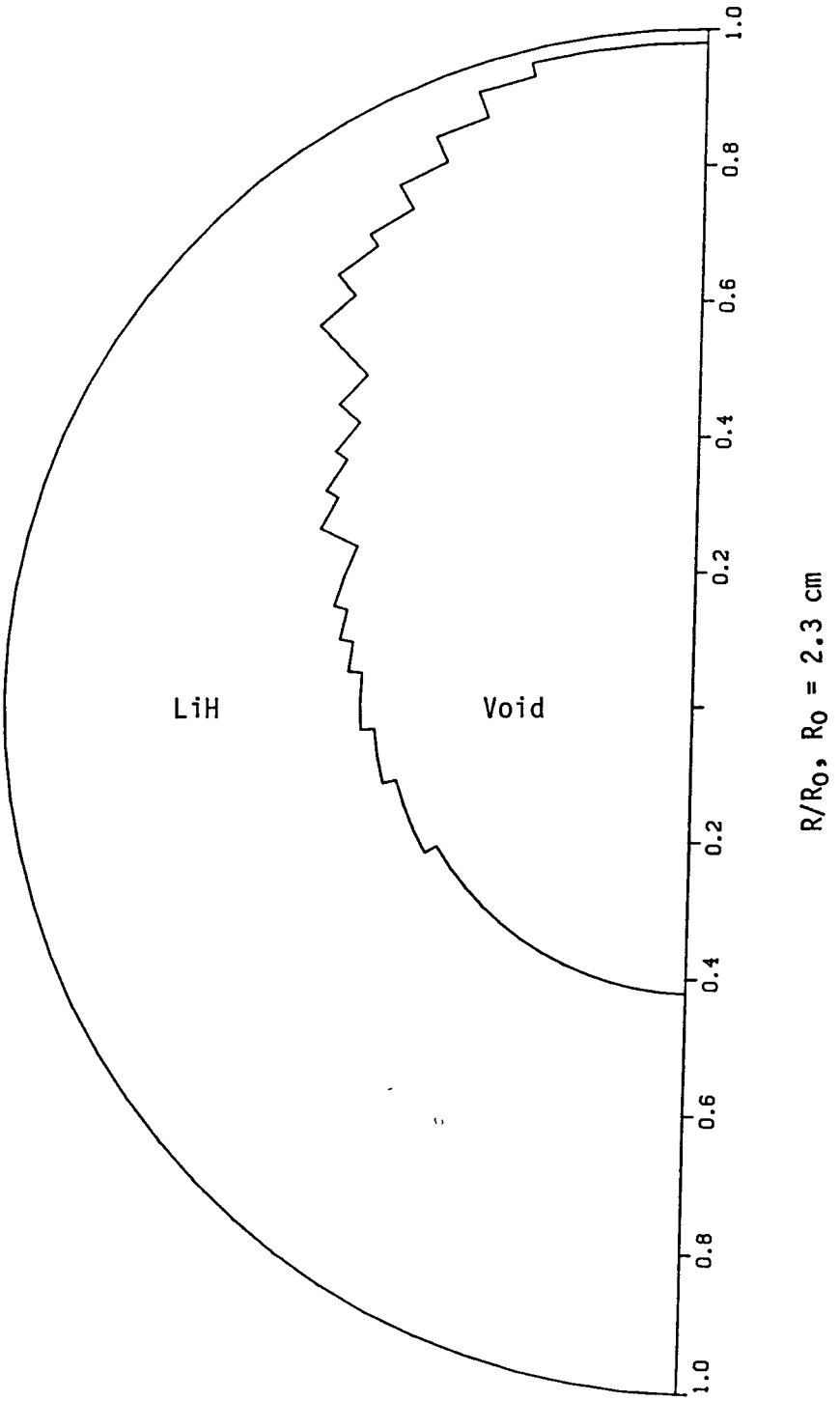

Fig. 8. Predicted lithium hydride freeze pattern for a slowly cooled 4.6 cm diameter sphere.

and about 10 L of heated volume. The size and power of the furnace will permit multiple sample testing.

Initial heatup tests were performed with the furnace in its current configuration to assess its performance capabilities. Data indicate that rapid heatups (~100 K/min) can be obtained in the induction furnace. It is anticipated that improvements in performance could be obtained by removing some of the thermal insulation, and reducing the susceptor wall thicknesses.

In order to estimate the thermal response of a sphere containing lithium hydride being heated in the furnace, a computer simulation was carried out assuming the furnace radiates as a blackbody initially at ambient temperature with the furnace temperature increasing at a rate of 100 K/min. Results indicate that while the average temperature of the solid lithium hydride in the high-flux furnace capsule is much higher than in the real case, much of the solid is cold enough to retain some significant mechanical strength. Thus, some of the stress-related problems previously discussed are likely to be observed in tests conducted in the high-flux furnace.

5. Conclusions

Based on preliminary value analysis, it was concluded that system storage densities of 3 MJ/kg or greater are required to produce significant mass savings in the heat rejection system. It is reasonable to expect operational storage densities in excess of this goal using the encapsulated lithium hydride packed-bed concept. The most promising

system uses Li-6 as the storage medium with a packing density of 75% and lithium as the thermal transport medium.

A group of feasibility issues associated with encapsulated lithium hydride thermal energy storage have been identified and discussed. The feasibility issues include:

1. phase-change induced shell stress on heatup,
2. hydrogen diffusion and loss,
3. lithium hydride heat transfer,
4. void behavior/management, and
5. material considerations.

The key issue of concern is the possible large shell stress induced during heatup. Elastic stress analysis indicates that very thick shells will be required to prevent shell rupture, assuming the lithium hydride forms a structurally sound shell following solidification. However, cracks in the lithium hydride which have been observed to form during cooldown, may mitigate shell stresses and permit the use of a thin shell. Nevertheless, analysis has shown that void control, via sphere heat transfer control, may lead to significantly reduced phase-change induced shell stress. Alternatively, a flexible shell, such as a bellows, may be viable.

Heat transfer considerations indicate that storage in a sphere with a maximum diameter of about 4 cm permits complete melting of the lithium hydride in 500 s, and thus provides maximum storage density.

Based on material consideration, 304L stainless steel and molybdenum are leading candidate shell materials. Material considerations included material compatibility between the shell and lithium hydride,

lithium, and hydrogen, ductility, strength, density, material cost, and ease of fabrication.

Based on projected system requirements, a 0.0127 cm (5 mil) 304L stainless steel shell will provide sufficient hydrogen containment to prevent significant hydrogen loss, and associated loss of storage density. Due to molybdenum's lower hydrogen permeability, a molybdenum shell as thin as 1 mil could be used without significant hydrogen loss.

Initial scoping experiments have been completed for cylindrical and spherical shells containing lithium hydride. Four thermal cycles were successfully completed in a low heat flux furnace with a cylindrical can with a 0.0889 cm (35-mil) wall thickness and one thermal cycle was successfully completed with a 0.0254 cm (10-mil) thick spherical container. Results of the thin-wall sphere test provide some confidence that a 0.0127-cm (5-mil) thick spherical shell can be used without suffering buckling failure. Post-test examination of all canisters tested showed the presence of numerous cracks in the lithium hydride.

Acknowledgments

This work was sponsored by the Air Force Wright Aeronautical Laboratories, AeroPropulsion Laboratory. The work was performed under Interagency Agreement DOE 40-1508-84. Extensive Y-12 Plant experience with lithium hydride was tapped to accomplish experimental objectives; W. L. Asbury, C. E. Irwin, and G. E. Wrenn have been particularly helpful.

References

1. Olszewski, M., and Morris, D. G., "Assessment of Energy Storage Concepts for Use in Pulsed Space Power Systems," Proceedings of 22nd Intersociety Energy Conversion Engineering Conference, Philadelphia, PA, August 10-14, 1987.

2. Morris, D. G., Foote, J. P. and Olszewski, M., "Development of Encapsulated Lithium Hydride Thermal Energy Storage for Space Power Systems," ORNL/TM-10413 (to be published)

3. Patankar, S. V., "Numerical Heat Transfer and Fluid Flow," Hemisphere Publishing Co., 1980.

4. Stewartson, K. and Waechter, "On Stefan's Problem for Spheres," Proc. R. Soc. Lond. A.348, 415-526 (1976).

5. Hsu, C. J., "Heat Transfer to Liquid Metals Flowing Past Spheres and Elliptical Rod Bundles," Int. J. Heat Mass Transfer," Vol. 8, 303-315 (1965).

6. Anon., "Nuclear Propulsion Program Engineering Progress Report," PWAC-604, Oct. 1-Dec. 31, 1960, Pratt and Whitney Aircraft Corp., Jan. 31, 1961, pp. 88-89.

7. Anon., "Nuclear Propulsion Program Engineering Progress Report," PWAC-611, Jan. 1-Mar. 31, 1961, Pratt and Whitney Aircraft Corp., Apr. 18, 1961.

8. Welch, Frank H., "Properties of Lithium Hydride III. Summary of GE-ANP Data," XDC-61-5-67, Aircraft Nuclear Prop. Dept., General Electric Co., May 1961, p. 7.

9. Hoke, John H., "Mechanical Properties of Stainless Steels at Elevated Temperatures," pp. 21-1 - 21-20 in Handbook of Stainless Steels, Peckner, Donald, and Bernstein, I. M., editors, McGraw-Hill Book Company, 1977.

10. Anon., "Refractory Metals and Custom Fabrication," Rembar Company, Inc.

11. Waldrop, F. B., "Lithium Hydride as a Mobile Neutron Shield," Y-1191, Union Carbide Nuclear Corp., February 24, 1958, p. 7-8.

12. Smith, Roger L., and Miser, James W., "Compilation of the Properties of Lithium Hydride," NASA-TM-X-483, 1962, p. 171-200.

13. Flint, P. S., "The Diffusion of Hydrogen Through Materials of Construction," Knolls Atomic Power Laboratory, KAPL-659, December 14, 1951.

14. Mahefkey, E. T., Air Force Weight Aeronautical Laboratories, AeroPropulsion Laboratory, Dayton, Ohio, personal communication to D. G. Morris, Oak Ridge National Laboratory, Martin Marietta Energy Systems, Inc., Oak Ridge, TN, January 1987.

15. TRW Power Systems Department, "Brayton Cycle Cavity Receiver Design Study," TRW Equipment Laboratories, NASA CR-54742 ER-6497, November 22, 1965.

16. Gnadt, P. A., "Filling Heat Storage Tubes for Solar Brayton-Cycle Heat Receiver With Lithium Fluoride," Oak Ridge National Laboratory, ORNL/TM-2732, July 1970.